Journal of Nepal Geological Society, 2025, Vol. 69, pp. 33-40
https://doi.org/10.3126/jngs.v69i1.88314

A boosting framework for slope unit-based earthquake-induced landslide susceptibility mapping

Suchita Shrestha[1] and *Tae-Seob Kang[2]

[1]Department of Mines and Geology, Ministry of Industry, Commerce and Supplies, Government of Nepal, Lainchour, Kathmandu, Nepal

[2]Division of Earth Environmental System Science, Pukyong National University, Busan, Republic of Korea

**Corresponding author's email: tskang@pknu.ac.kr*

ABSTRACT

In mountainous areas, landslides brought on by earthquakes are a major threat to infrastructure, human life, and sustainable development. Thousands of landslides were caused by the 2015 Mw 7.8 Gorkha earthquake in Nepal, underscoring the critical need for trustworthy techniques to pinpoint regions most susceptible to seismically induced slope failures. In the Sindhupalchowk District, one of the areas most severely impacted by earthquakes, this study suggests a boosting-based framework for mapping landslide susceptibility using slope units. Twelve geophysical covariates representing terrain, hydrological, geological, and seismic conditions were integrated with a thorough landslide inventory comprising 7,159 earthquake-induced landslides. In contrast to traditional grid-based methods, slope units were employed as mapping units to more accurately depict geomorphological processes. The boosting model was trained using 70% of the dataset and validated with the remaining 30%. The receiver operating characteristic curve was one of several statistical metrics used to assess the model's performance. With an area under the curve value of 0.83, the results demonstrate strong predictive capability and good discrimination between slope units that are prone to landslides and those that are stable. High-risk areas are concentrated along steep slopes, deeply carved valleys, and regions that experience severe ground shaking, according to the resulting susceptibility map. Overall, in seismically active mountainous areas, the suggested framework offers a reliable and comprehensible method for evaluating landslide susceptibility to earthquakes and offers insightful information to support hazard mitigation, land-use planning, and disaster risk reduction.

Keywords: Landslide; Slope unit; Boosting model; Validation

Received: 16 July 2025 **Accepted:** 15 December 2025

INTRODUCTION

Landslides are among the most catastrophic natural hazards globally, causing substantial financial loss and hundreds of deaths and injuries each year (Crozier and Glade, 2012). Landslides caused by earthquakes are known to be a major natural hazard, in some cases causing as much or more damage than the initial ground shaking. On 25 April 2015, a catastrophic earthquake of Mw 7.8 was struck Nepal at 06:11:26 UTC. The epicenter of the main shock was located at Barpak, (28°15′07″ N, 84°07′02″ E) in the Gorkha District, approximately 75 km east of Kathmandu. The earthquake killed more than 9000 people, and fully or partially damaged 1.1 million houses. Over 400 aftershocks of ≥Mw 4 were recorded within two years after the main quake. The earthquake also triggered various mass movements, some of which caused damage, such as blocked roads and dammed rivers, and threatened infrastructures in many parts of the earthquake-affected areas with steep topography and deep valleys.

Large earthquakes frequently set off numerous landslides (Keefer 1984) and Gorkha earthquake was no exception. The earthquake and its aftershocks triggered thousands of landslides and some avalanches in the mountainous areas of Nepal with rugged topography, high relief, steep slopes and deep valleys (Collins and Jibson, 2015; Regmi et al. 2016). These significantly impacted the lives and economy of Nepal, the majority of which occurred between the epicenter of the mainshock and that of the May 12 aftershock. The main consequences of landslides resulting from this earthquake and its aftershocks were fatalities, property loss, river flow blockage, and damage to infrastructural systems. Shaking induced by previous events might weaken slopes (by opening joints in rock masses, fracturing materials, increasing pore water pressure in soil slopes, reducing cohesion in soils, etc.). The effects can cause slopes to fail in subsequent earthquakes, even under low-intensity events.

There are differing viewpoints among researchers regarding the identification of the most accurate prediction methodology or a combination of methods (Moayedi and Dehrashid, 2023). The reliability of landslide assessment in a particular area depends on the data quality used and the modeling method applied (Pradhan et al. 2023). The utilization of machine learning methodologies in research focused on Nepal's mountainous regions has been restricted primarily due to inadequate historical landslide datasets and current geospatial data. Furthermore, the present findings are independent and have not been incorporated into global or state databases.

During the past two decades, several models for landslide susceptibility mapping have been published, assuming that landslides occur in settings analogous to prior landslides and may be evaluated given the causative link is recognized (Liu

et al. 2023; Lombardo et al. 2018; Pradhan et al. 2016). These approaches are classified into two types: qualitative methods and quantitative methods.

The main objective of this study is to assess earthquake-induced landslide susceptibility in Sindhupalchowk District, central Nepal, using a boosting framework. The research focuses on capturing the nonlinear relationships between earthquake-related and terrain conditioning factors and the occurrence of landslides triggered by seismic events. The boosting is implemented within a geographic information system (GIS) user interface to support efficient data preparation, susceptibility map generation, and visualization. Model performance is evaluated using established validation techniques and statistical accuracy metrics. The resulting susceptibility map is intended to support earthquake risk mitigation, landuse planning, and disaster management in seismically active mountainous regions.

Study area And earthquake-induced landslides

The Sindhupalchowk District is located in central Nepal (85.44–86.06E and 27.61–28.20N) at an elevation of 750–7080 meter above sea level (masl) and covers about 2542 Km^2. The yearly rainfall is about 2500 mm, and the average temperature ranges from 7.5 degree to 32° Celsius. The region is hilly and full of rich resources in which majority of the population depend on agriculture for a livelihood. The region has a moderate slope with agricultural land, followed by woods with higher slope angles in the upper hills (Shrestha et al. 2017a). The district is known for its mountainous terrain, beautiful landscapes, and cultural diversity. The 2015 Nepal earthquake affected the district severely, causing widespread damage and loss of life. Reconstruction efforts are still underway in the area. Figure 1a depicts map showing the location of Sindhupalchowk District, Nepal.

A landslide inventory map is essential for examining the relationship between landslide occurrence and covariates. Such a map records the geographic locations of past landslides along with information on their type, size, and other distinguishing characteristics (Einstein, 1988). It therefore provides a fundamental basis for analyzing how landslides are distributed in relation to potential risk factors (Ma et al. 2025). In this study, 7159 landslides were identified by integrating information from previous reports, satellite imagery, and field surveys (Fig. 1b).

Geophysical covariates: landscape characteristics and ground motion data

This section describes the covariates used to explain the variability in the distribution of co-seismic landslide areas across the affected Sindhupalchowk District. Geophysical covariates are the terrain and environmental attributes that influence the balance between driving and resisting forces governing landslide movement (Pradhan and Kim, 2014; Shrestha et al. 2017a, 2017b). These factors define the underlying conditions that make a slope prone to failure. When such conditions are favorable, landslides are initiated in response to one or more triggering mechanisms. Since landslide occurrence is strongly controlled by topographic, hydrological, seismic, and geological characteristics.

In this work, 12 landslide geophysical covariates (Table 1, Figs. 2a, b, c, d, e, f, g, h, and i) typically reported in the literature were initially produced based on the assessment of the landslide inventory plot. We used a 20 m resolution digital elevation model (DEM) from Department of Survey, Government of Nepal. From this DEM, we derived a set of basic terrain attributes, including elevation, slope, curvature, topographic position index (TPI), topographic wetness index (TWI), stream power index (SPI), and sediment transport index (STI). Similarly, drainage proximity and drainage density were derived from Euclidian distance algorithm in GIS. Whereas, geological data was obtained from Department of Mines and Geology (DMG, 2020) and fault proximity was obtained from fault and thrust lines of geological map and Euclidian distance algorithm. The peak ground acceleration (PGA) data of the 2015 Gorkha earthquake were obtained from the US Geological Survey (USGS, 2015).

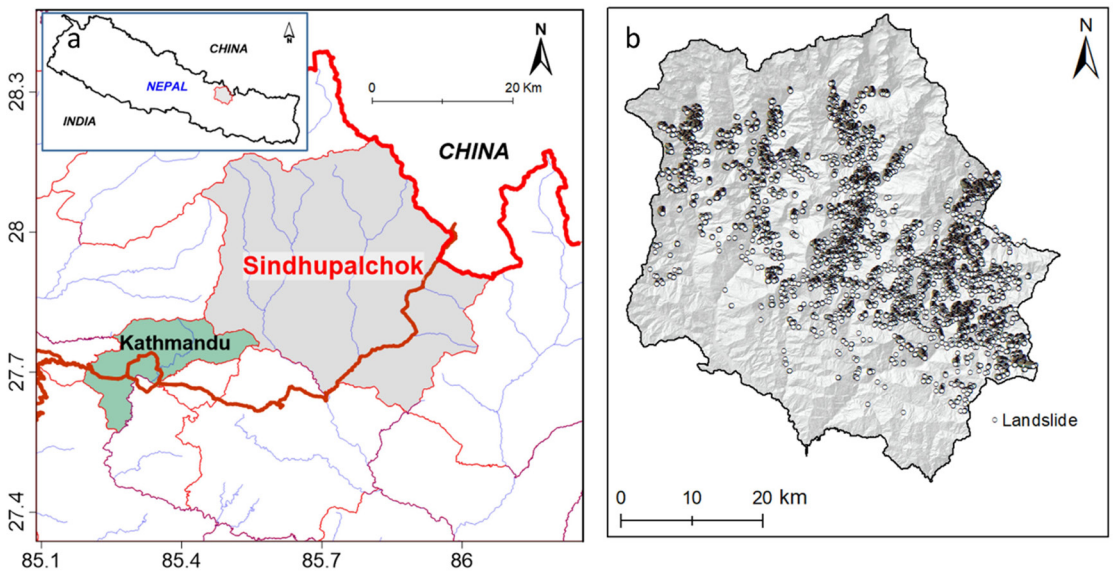

Fig. 1: a) Location map of Sidhnupalchowk district, and b) landslide distribution.

Table 1: Selected geophysical covariates and its significance.

Geophysical covariates	Its significance
Elevation	Elevation controls climatic conditions, vegetation cover, weathering intensity, and seismic wave amplification, all of which influence slope instability during earthquakes.
Slope	Slope angle is a primary controlling factor, as steeper slopes experience higher shear stress and are more susceptible to seismic shaking–induced failure.
Curvature	Surface curvature affects stress concentration and drainage behavior; convex slopes tend to amplify seismic forces, while concave slopes favor material accumulation and saturation.
TPI	TPI distinguishes ridges, mid-slopes, and valleys; ridges and upper slopes often experience stronger ground motion amplification during earthquakes.
Drainage proximity	Areas close to streams are prone to toe erosion and higher pore-water pressure, which reduce slope stability when subjected to seismic shaking.
Drainage density	High drainage density indicates intense surface dissection and weaker slope materials, increasing susceptibility to earthquake-triggered failures.
TWI	TWI represents potential soil moisture accumulation; saturated soils are more vulnerable to strength loss under cyclic seismic loading.
SPI	SPI reflects erosive power of flowing water, which weakens slope toes and predisposes slopes to failure during earthquakes.
STI	STI indicates sediment movement potential on slopes; areas with high sediment transport are often mechanically unstable under seismic excitation.
Geology	Lithology and structural conditions govern material strength, degree of fracturing, and weathering, strongly influencing landslide response to seismic shaking.
Fault proximity	Proximity to active faults increases ground motion intensity and permanent ground deformation, making nearby slopes highly susceptible to earthquake-induced landslides.
PGA	PGA directly represents seismic shaking intensity; higher PGA values significantly increase the likelihood of slope failure during earthquakes.

MAPPING UNITS

Slope Units (SU) are more adept at accurately capturing the geophysical covariates conducive to landslide formation, signifying their geological importance (Ma et al. 2023). The SU concept pertains to terrain segments delineated by drainage and divide lines. SU offers a solution to address the limitation of Grid Units (GU) analyses, as highlighted by Tanyas et al. (2019). This study utilized the R-statistical programming language (Pradhan et al. 2025; Yu and Chen, 2020) for hydrological analysis using DEM data to define hydrological "half-basin" boundaries.

The resulting SUs provided a medium-resolution representation of the Sindhupalchowk district (Fig. 3), comprising a total of 4,184 SU. The planimetric area of these SUs has a mean value of 0.59 km², with a standard deviation of 0.53 km². Out of 4,184, 1390 SU contains landslides.

METHODOLOGY

The methodology depicted in the flowchart (Fig. 4) outlines a systematic machine learning approach for modeling earthquake-induced landslide susceptibility. The process begins by integrating two primary data sources: a landslide inventory, and geophysical covariates. These inputs are mapped onto a SU framework, which serves as the primary terrain subdivision for analysis.

To develop and validate the predictive model, the integrated dataset is partitioned into a 70% training set to calibrate the algorithm and a 30% test set for independent evaluation. These data subsets are processed through a boosting model. Following the modeling phase, an accuracy assessment is performed to verify the performance of the algorithm against the test data. The final output of this workflow is a susceptibility map or index that identifies areas most prone to landslides triggered by seismic activity.

In the context of earthquake-induced landslide susceptibility, the boosting method is an iterative ensemble learning technique that enhances predictive performance by sequentially combining multiple "weak" learners, typically simple decision trees to form a robust "strong" model. Unlike parallel methods that build independent models, boosting trains each new tree to specifically minimize the residual errors of its predecessor, effectively "boosting" the importance of SUs that were previously misclassified or difficult to predict. This sequential refinement is particularly advantageous for earthquake-induced

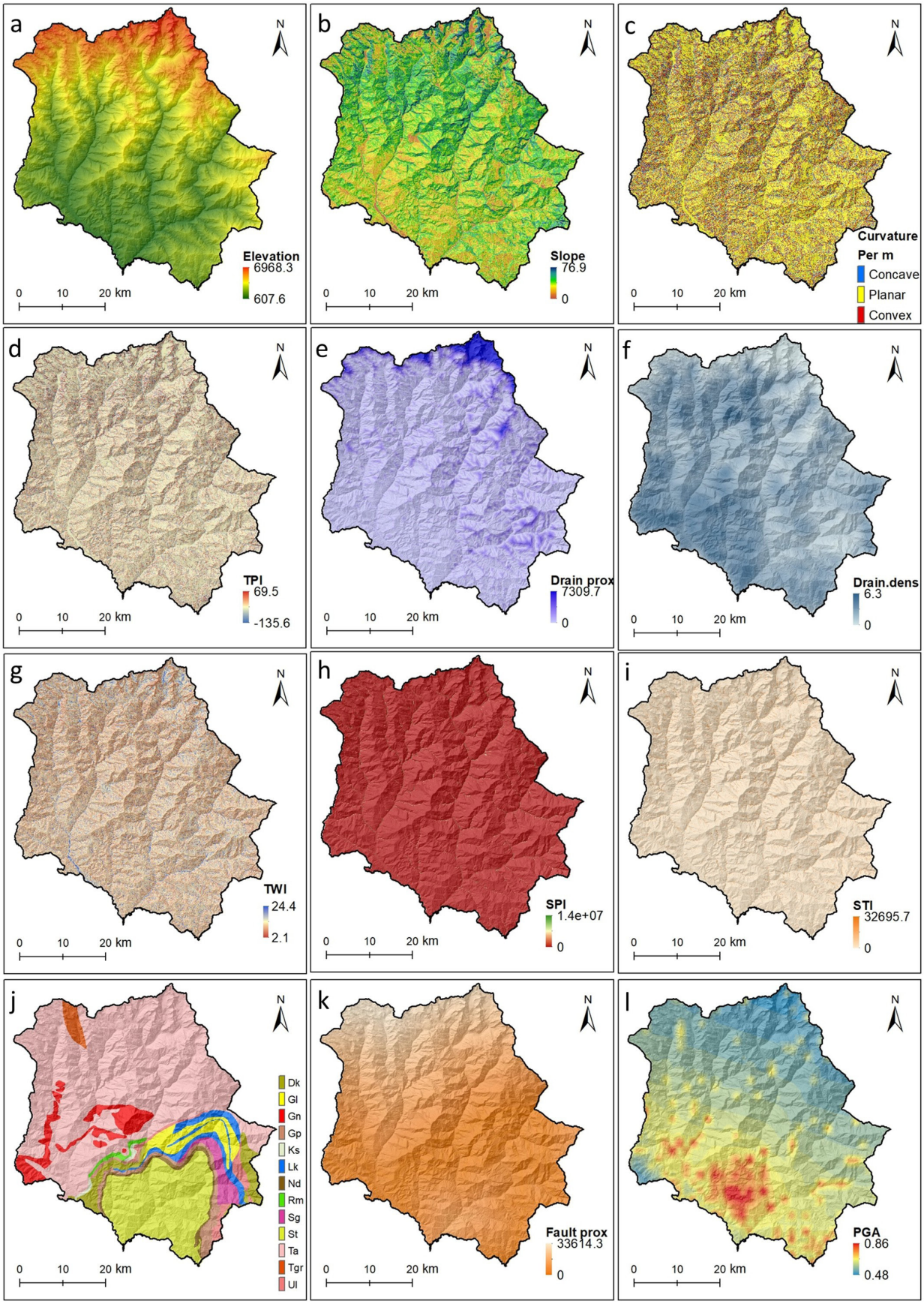

Fig. 2: Example of geophysical covariates used for the analysis.

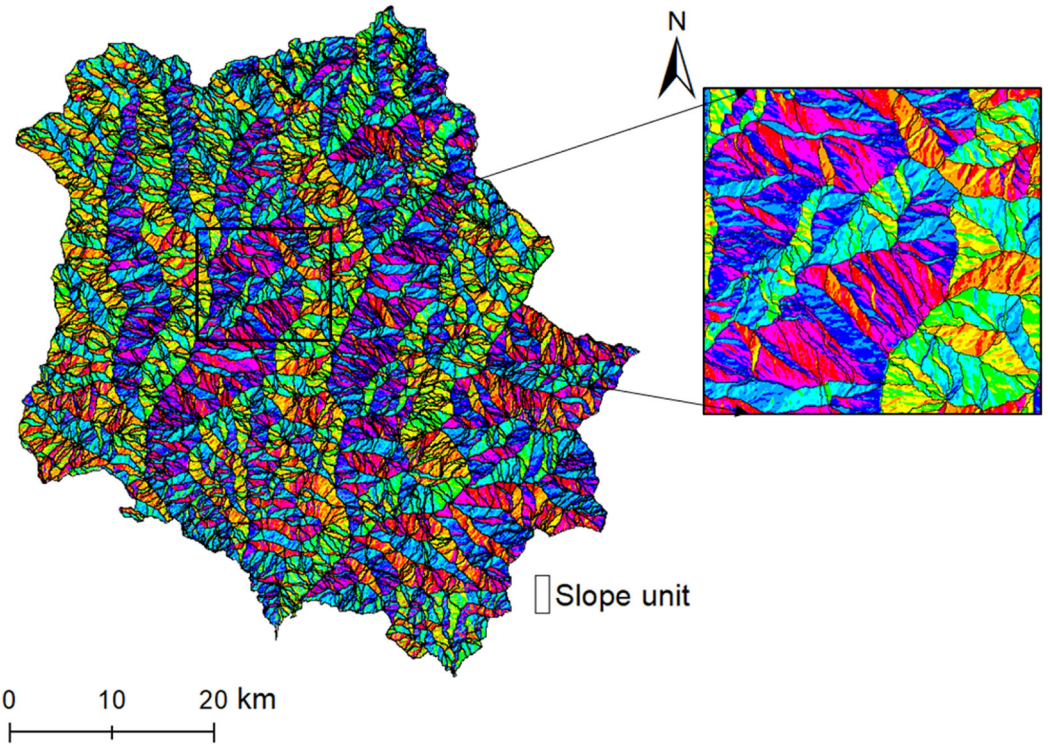

Fig. 3: SU distribution in the study area.

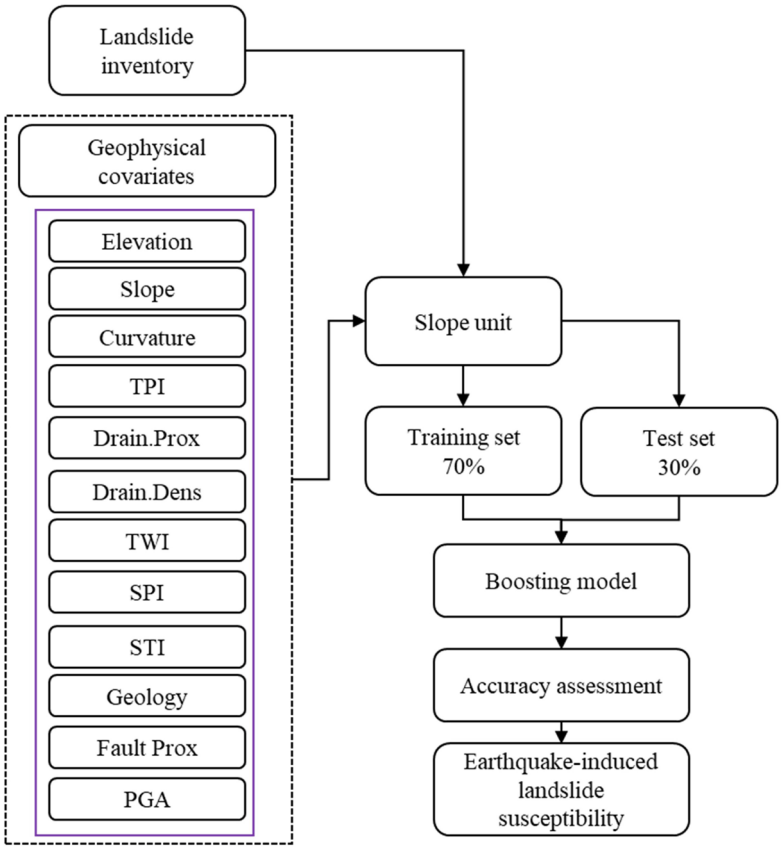

Fig. 4: Methodological framework of the study.

landslide modeling because it can capture the complex, non-linear interactions between static terrain factors (like slope and curvature) and dynamic seismic triggers (like PGA).

The core idea of most model evaluation procedures involves spliting the dataset into training and test sets. The training set was used to fit the model, which was subsequently applied to the test set to evaluate its predictive capabilities. Out of 4184 SUs, 70% (2929 SUs) were subjected to the training the model and 30% (1255 SUs) were for the test the model. A The results were systematically organized into a confusion matrix, which presents a detailed breakdown of the predictions across four categories: False Positives (FP), False Negatives (FN), True Positives (TP), and True Negatives (TN). A summary and explanation of each metric is given in Table 1. The performance of the model was evaluated using a variety of standard evaluation metrics as given in Table 2.

Table 2: Model performance matrices.

Matrices	Equation	Meaning
F1 Score	(2 × Precison × Recall)/(Precision + Recall), where Precision= TP/(TP + FP) and Recall= TP/(TP + FN)	The harmonic mean of precision and recall and provides a balanced measure of classification performance, especially useful for imbalanced datasets
True Negative Rate	TNR=TN/TN+FP	Referred to as specificity, measures the proportion of non-landslide units correctly classified as non-landslide
False Negative Rate	FNR=FN/FN+TP	Quantifies the proportion of landslide-affected units that are incorrectly classified as non-landslide.

RESULTS

Landslide predictive map

The boosting-based model successfully generated an earthquake-induced landslide susceptibility map for the Sindhupalchowk District using SUs as the mapping framework (Fig. 6). The final susceptibility map shows a clear spatial differentiation of landslide-prone areas, with high and very high susceptibility zones predominantly concentrated along steep slopes, deeply incised valleys, and regions subjected to strong ground shaking during the 2015 Gorkha earthquake. These zones align well with the observed distribution of co-seismic landslides, indicating that the model effectively captured the combined influence of terrain characteristics and seismic forcing.

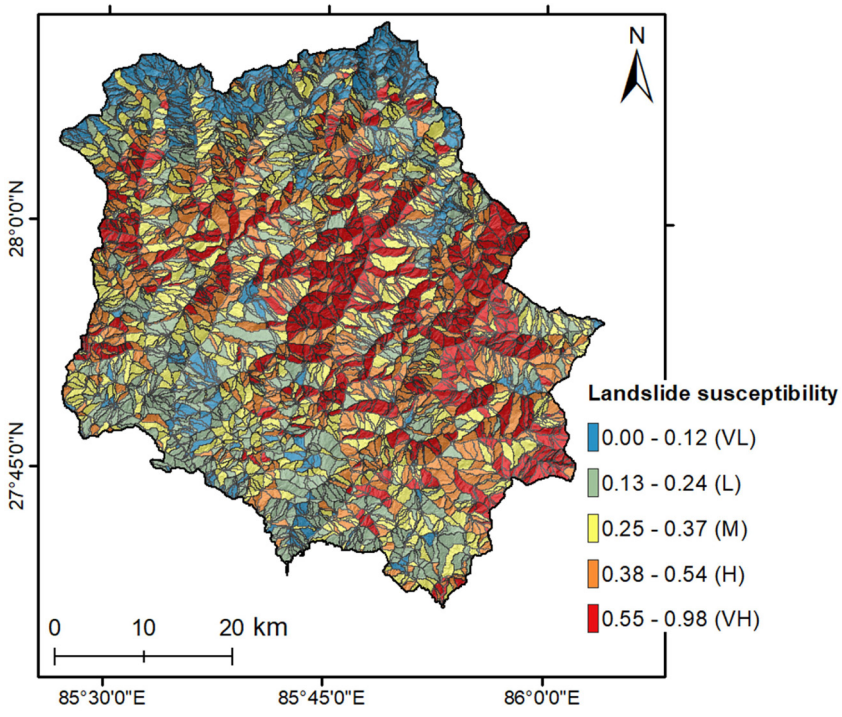

Fig. 6: Earthquake-induced landslide susceptibility

Model performance was evaluated using several statistical metrics derived from the independent test dataset. The receiver operating characteristic (ROC) curve demonstrates strong discriminative capability, with an area under the curve (AUC) value of 0.83, indicating good overall predictive accuracy (Fig. 7). This result confirms that the boosting framework can reliably distinguish between SUs with and without landslide occurrences. The F1 score of 0.642 further reflects a balanced performance between precision and recall, suggesting that the model is effective in identifying landslide-prone SUs while limiting misclassification (Table 3).

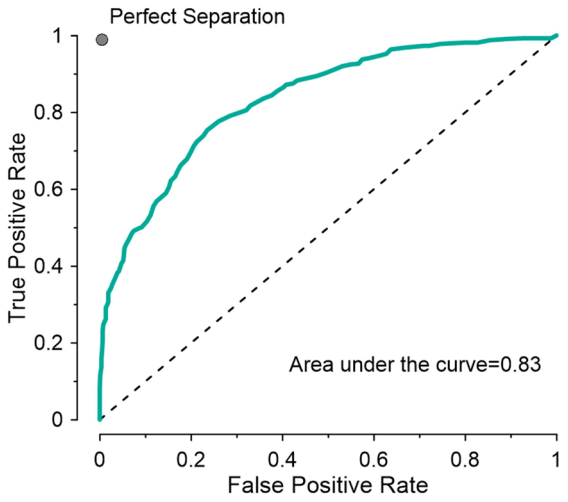

Fig. 7: ROC curves plot.

Table 3: Model performance matrices and corresponding value

Matrices	Value
F1 Score	0.642
True Negative Rate	0.855
False Negative Rate	0.387

Additional performance indicators support the robustness of the model. The true negative rate of 0.855 and negative predictive value of 0.818 indicate that SUs classified as stable are, in most cases, correctly identified. Although the false negative rate is relatively moderate (0.387), the overall threat score of 0.626 suggests a reasonable capability of the model to capture actual landslide occurrences. The statistical parity value of 0.299 indicates some imbalance between predicted classes, which is expected given the inherent imbalance between landslide-affected and non-affected SUs.

The out-of-bag improvement plot illustrates a steady enhancement in model performance with successive boosting iterations (Fig. 8), confirming that each additional learner contributes to reducing prediction errors. This behavior highlights the advantage of the boosting approach in progressively refining model accuracy by focusing on previously misclassified SUs.

Furthermore, the relative influence plot reveals that seismic and topographic variables play dominant roles in controlling landslide susceptibility as shown in Fig. 9. Peak ground acceleration and slope-related parameters exhibit the highest influence, followed by terrain indices linked to hydrological

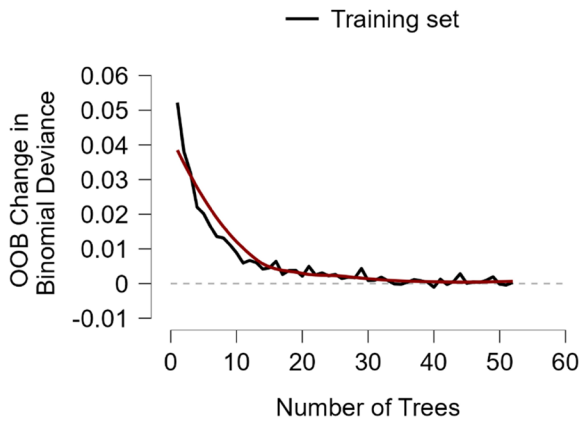

Fig. 8: Out-of-bag improvement plot

conditions and geomorphic positioning, emphasizing the combined role of seismic triggering and terrain predisposition in earthquake-induced landsliding.

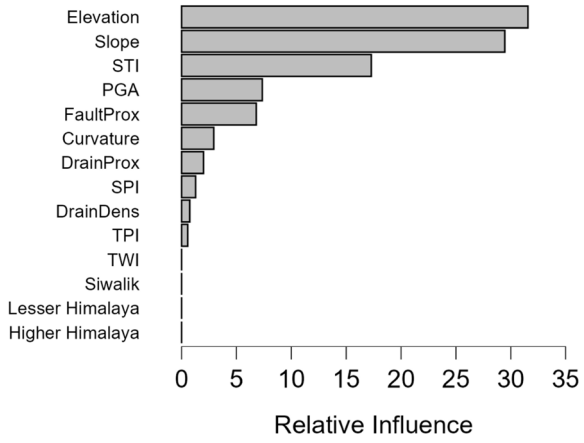

Fig. 9: Relative influence plot.

DISCUSSION

The results of this study indicate that the boosting-based framework is well suited for earthquake-induced landslide susceptibility mapping in the mountainous terrain of Sindhupalchowk District. The spatial agreement between high-susceptibility zones and the observed distribution of co-seismic landslides suggests that the model effectively captured the combined influence of seismic triggering and terrain-controlled preconditioning factors. This supports the applicability of boosting algorithms for representing the complex, non-linear relationships involved in landslide initiation during strong earthquakes.

The model achieved good predictive performance, with an AUC value of 0.83, demonstrating its ability to distinguish between landslide-affected and stable slope units. The iterative learning mechanism of boosting, which emphasizes previously misclassified units, contributed to improved classification accuracy compared to single-model approaches. This advantage is particularly important in seismically active regions, where landslide occurrence is governed by the interaction of ground motion intensity and terrain characteristics.

The SU-based approach further enhanced model reliability by providing geomorphologically meaningful mapping units that better reflect landslide processes than conventional grid cells. Relative influence analysis identified peak ground acceleration and slope-related parameters as the most influential predictors, confirming the dominant role of seismic shaking and topographic controls. However, the moderate false negative rate highlights the influence of inventory uncertainties and the lack of detailed geotechnical data. Future studies could address these limitations by integrating additional subsurface information and advanced strategies for handling class imbalance.

CONCLUSIONS

This study presents a boosting-based framework for earthquake-induced landslide susceptibility mapping using slope units in the Sindhupalchowk District of central Nepal. The results demonstrate that the proposed approach effectively captures the complex interactions between seismic triggering factors and terrain conditioning variables. The generated susceptibility map shows strong spatial agreement with observed co-seismic landslides from the 2015 Gorkha earthquake, confirming the reliability of the model for regional-scale hazard assessment. Model validation indicates good predictive performance, with an AUC value of 0.83, highlighting the advantage of boosting algorithms in handling non-linear relationships and heterogeneous geophysical conditions. The slope unit-based representation further improves process realism by aligning mapping units with geomorphological and hydrological boundaries. Relative influence analysis emphasizes the dominant role of peak ground acceleration and slope-related parameters in controlling landslide occurrence.

ACKNOWLEDGEMENT

This work was supported by the Global Joint Research Program funded by the Pukyong National University (202412180001).

All views and interpretations expressed in this publication are those of the authors and are not necessarily attributable to Department of Mines and Geology, Ministry of Industry, Commerce and Supplies, Government of Nepal.

REFERENCES

Chigira, M., Wu, X., Inokuchi, T., Wang, G., 2010. Landslides Chigira, M., Wu, X., Inokuchi, T., and Wang, G., 2010, Landslides induced by the 2008 Wenchuan earthquake, Sichuan, China. Geomorphology, v. 118, pp. 225–238. https://doi.org/10.1016/j.geomorph.2010.01.003.

Collins, B., and Jibson, R.,2015, Assessment of existing and potential landslide hazards resulting from the April 25, 2015 Gorkha, Nepal earthquake sequence.

Crozier, M.J., and Glade, T., 2012, Landslide Hazard and Risk: Issues, Concepts and Approach, in: Landslide Hazard and Risk, pp. 1–39. https://doi.org/10.1002/9780470012659.ch1

DMG, 2020, Department of Mines and Geology, Ministry of Industry, Commerce and Supplies. dmgnepal.gov.np.

Einstein, H.H., 1988, Special lecture: landslide risk assessment procedure, Landslides. Proc. 5th symposium, Lausanne, 1988, V. 2.

Keefer, D.K., 1984, Landslides caused by earthquakes. Geol. Soc. Am. Bull., v. 95, pp. 406–421. https://doi.org/10.1130/0016-7606.

Liu, S., Wang, L., Zhang, W., He, Y., and Pijush, S., 2023, A comprehensive review of machine learning-based methods in landslide susceptibility mapping. Geol. J., v. 58, pp. 2283–2301.

Lombardo, L., Opitz, T., and Huser, R., 2018, Point process-based modeling of multiple debris flow landslides using INLA: an application to the 2009 Messina disaster. Stoch. Environ. Res. Risk Assess., v. 32, pp. 2179–2198. https://doi.org/10.1007/s00477-018-1518-0.

Ma, S., Shao, X., and Xu, C., 2025, Landslide inventory and distribution patterns in Lhasa area, Tibet Plateau. Nat. Hazards, v. 121, pp. 5849–5871. https://doi.org/10.1007/s11069-024-07031-z.

Ma, S., Shao, X., and Xu, C., 2023, Landslide Susceptibility Mapping in Terms of the Slope-Unit or Raster-Unit, Which is Better? J. Earth Sci., v. 34, pp. 386–397. https://doi.org/10.1007/S12583-021-1407-1/METRICS.

Moayedi, H., and Dehrashid, A.A., 2023, A new combined approach of neural-metaheuristic algorithms for predicting and appraisal of landslide susceptibility mapping. Environ. Sci. Pollut. Res., v. 30, pp. 82964–82989.

Pradhan, A.M.S., Ghimire, P., Shrestha, S., Lee, J.-S., Lee, J.-H., and Park, H.-J., 2025, Extreme gradient boosting with Shapley Additive Explanations for landslide susceptibility at slope unit and hydrological response unit scales. Geosci. Front., v. 16, pp. 102081.

Pradhan, A.M.S., Kang, H.-S., Lee, S., and Kim, Y.-T., 2016, Spatial model integration for shallow landslide susceptibility and its runout using a GIS-based approach in Yongin, Korea. Geocarto Int., pp. 1–55. https://doi.org/10.1080/10106049.2016.1155658.

Pradhan, A.M.S., and Kim, Y.T., 2014, Relative effect method of landslide susceptibility zonation in weathered granite soil: A case study in Deokjeok-ri Creek, South Korea. Nat. Hazards, v. 72, 1189–1217. https://doi.org/10.1007/s11069-014-1065-z.

Pradhan, B., Dikshit, A., Lee, S., and Kim, H., 2023, An explainable AI (XAI) model for landslide susceptibility modeling. Appl. Soft Comput., pp. 110324.

Qi, S., Xu, Q., Lan, H., Zhang, B., and Liu, J., 2010, Spatial distribution analysis of landslides triggered by 2008.5.12 Wenchuan Earthquake, China. Eng. Geol., v. 116, pp. 95–108. https://doi.org/10.1016/j.enggeo.2010.07.011.

Regmi, A.D., Dhital, M.R., Zhang, J., Su, L., and Chen, X., 2016, Landslide susceptibility assessment of the region affected by the 25 April 2015 Gorkha earthquake of Nepal. J. Mt. Sci., v. 13, pp. 1941–1957. https://doi.org/10.1007/s11629-015-3688-2.

Shrestha, S., Kang, T.-S., and Suwal, M., 2017, An Ensemble Model for Co-Seismic Landslide Susceptibility Using GIS and Random Forest Method. ISPRS Int. J. Geo-Information, v. 6, p. 365. https://doi.org/10.3390/ijgi6110365.

Tanyas, H., Rossi, M., Alvioli, M., van Westen, C.J., and Marchesini, I., 2019, A global slope unit-based method for the near real-time prediction of earthquake-induced landslides. Geomorphology, v. 327, pp. 126–146. https://doi.org/10.1016/J.GEOMORPH.2018.10.022.

USGS, 2015, The M7.8 Nepal Earthquake, 2015 – A Small Push to Mt. Everest [WWW Document].

Yin, Y., Wang, F., and Sun, P., 2009, Landslide hazards triggered by the 2008 Wenchuan earthquake, Sichuan, China. Landslides, v. 6, pp. 139–151. https://doi.org/10.1007/s10346-009-0148-5.

Yu, C., and Chen, J., 2020, Application of a GIS-Based Slope Unit Method for Landslide Susceptibility Mapping in Helong City: Comparative Assessment of ICM, AHP, and RF Model. Symmetry 2020, v. 12, pp. 1848 12, 1848. https://doi.org/10.3390/SYM12111848.